



**Michigan  
Technological  
University**

Michigan Technological University  
**Digital Commons @ Michigan Tech**

---

Michigan Tech Publications, Part 2

---

8-2024

## Evidence for rapid variability at high energies in GRBs

E. Casey Aldrich

*Michigan Technological University*, [ecaldric@mtu.edu](mailto:ecaldric@mtu.edu)

Robert J. Nemiroff

*Michigan Technological University*, [nemiroff@mtu.edu](mailto:nemiroff@mtu.edu)

Follow this and additional works at: <https://digitalcommons.mtu.edu/michigantech-p2>



Part of the [Physics Commons](#)

---

### Recommended Citation

Aldrich, E., & Nemiroff, R. J. (2024). Evidence for rapid variability at high energies in GRBs. *Monthly Notices of the Royal Astronomical Society*, 532(2), 2674-2682. <http://doi.org/10.1093/mnras/stae1573>  
Retrieved from: <https://digitalcommons.mtu.edu/michigantech-p2/917>

Follow this and additional works at: <https://digitalcommons.mtu.edu/michigantech-p2>



Part of the [Physics Commons](#)

# Evidence for rapid variability at high energies in GRBs

E. Casey Aldrich<sup>★</sup> and Robert J. Nemiroff<sup>✉★</sup>

*Michigan Technological University, Dept. of Physics, 1400 Townsend Dr., Houghton, MI, USA*

Accepted 2024 June 20. Received 2024 June 5; in original form 2024 March 15

## ABSTRACT

Intrinsic variability was searched for in arrival times of six gamma-ray bursts (GRBs) at high energies – between 30 MeV and 2 GeV – detected by the *Fermi* satellite’s Large Area Telescope (LAT). The GRBs were selected from the *Fermi* LAT catalogue with preference for events with numerous photons, a strong initial pulse, and measured redshifts. Three long GRBs and three short GRBs were selected and tested. Two different variability-detection algorithms were deployed, one counting photons in pairs, and the other multiplying time gaps between photons. In both tests, a real GRB was compared to 1000 Monte Carlo versions of itself smoothed over a wide range of different time-scales. The minimum detected variability time-scales for long bursts (GRB 080916C, GRB 090926A, GRB 131108A) was found to be (0.005, 10.0, 10.0) s for the photon pair test and (2.0, 20.0, 10.0) s for the time-gap multiplication test. Additionally, the minimum detected variability time-scales for the short bursts (GRB 090510, GRB 140619B, GRB 160709A) was found to be (0.05, 0.01, 20.0) s for the photon pair test and (0.05, 0.01, 20.0) s for the gap multiplication test. Statistical uncertainties in these times are about a factor of 2. The durations of these variability time-scales may be used to constrain the geometry, dynamics, speed, cosmological dispersion, Lorentz-invariance violations, weak equivalence principle violations, and GRB models.

**Key words:** methods: data analysis – methods: statistical – gamma-ray burst: general.

## 1 INTRODUCTION

Gamma-ray bursts (GRBs) are among the most distant known transient events, with redshifts typically greater than one (Zitouni et al. 2018) and as great as (estimated) redshift 9 (Cucchiara et al. 2011). A comprehensive living list of GRBs with both measured and estimated redshifts is provided by Greiner (2024). The significant distance to GRBs can provide valuable scientific insights into various aspects of the young universe, such as early stellar evolution, star formation rates, and the physics of the early cosmological epochs. For a good review of GRBs, see Levan (2018).

Along with fast radio bursts, GRBs are among the shortest-duration astronomical events known. GRBs have measured durations ranging from milliseconds to hours at gamma-ray energies (Norris et al. 1995; MacLachlan et al. 2012). GRBs are often characterized by constituent pulses that are dominated by a relatively rapid rise and slow decay, which have been extensively studied (Desai 1981; Norris et al. 1996; Ryde & Svensson 2002; Nemiroff 2012). Broad temporal characteristics of GRBs are important for providing insights into the internal physics and kinematics of these phenomena (Piran 2004).

GRBs are commonly categorized as either long or short, based on their duration and spectral properties (Kouveliotou et al. 1993; Shahmoradi & Nemiroff 2015). Long GRBs typically last for more than 2 s and exhibit relatively soft spectra. A prevailing progenitor model for these events involves a core-collapse supernova that occurs when a massive star depletes the fusible elements in its core

(Woosley & Bloom 2006). In contrast, short GRBs generally have durations of less than 2 s and are characterized by harder spectra. The dominant progenitor model for short GRBs posits that they result from a kilonova, which is associated with the merger of two neutron stars that eventually form a black hole (Eichler et al. 1989).

The contemporary GRB detector most sensitive to individual photons near 100 MeV (hereafter called ‘high-energy’) is the Large Area Telescope (LAT; Atwood et al. 2009) aboard the *Fermi* Gamma-Ray Space Telescope (*Fermi*). The *Fermi* LAT primarily detects gamma-ray photons between 20 MeV and 10 GeV. A summary of GRB events can be found in the *Fermi* LAT’s First and Second GRB Catalogues (Ackermann et al. 2013; Ajello et al. 2019). In the decade from mid-2008 to mid-2018, the *Fermi* LAT recorded 186 GRBs with a significant excess of photons (Ajello et al. 2019). In comparison, during this time, the *Fermi* Gamma-ray Burst Monitor (GBM), which detects gamma-rays between 8 keV and 40 MeV (hereafter called ‘low-energy’) – but mostly at the lower end – triggered on 2357 GRBs (Ajello et al. 2019), indicating that relatively few GRBs emit a significant excess of LAT-detectable high-energy photons. However, in contrast with the GBM, individual photons detected by the LAT that are time and direction related to a GRB have a high confidence of being actually GRB photons – and not from a pervasive background.

Rapid variability in the prompt gamma-ray emission of GRBs has been searched for many times and with different methods, but mostly at the lower photon energies detectable by GBM. Millisecond variability was detected at near the 100 keV energy scale (Bhat et al. 1992; Schaefer 1999). Walker, Schaefer & Fenimore (2000) searched the initial 1 s of many Burst and Transient Source Experiment

\* E-mail: [ecaldric@mtu.edu](mailto:ecaldric@mtu.edu) (EA); [nemiroff@mtu.edu](mailto:nemiroff@mtu.edu) (RN)

(BATSE) GRBs in the energy range 25 keV to 1 MeV and found that 30 percent showed a rise-time variability of less than 1 ms. None of these GRBs, though, had a known redshift.

MacLachlan et al. (2012) analysed pulses that occurred in both short GRBs and long GRBs detected by the GBM with a wavelet analysis and found variability time-scales between 0.001 and 0.01 s as well as a temporal offset between short and long GRBs. Subsequently, MacLachlan et al. (2013) studied GBM bursts using a wavelet analysis and found several short GRBs that have a variability time-scale between 0.001 and 0.01 s, as well as several long GRBs with variability time-scales from 0.01 to 1 s. Variability time-scale has also been used to estimate the size of the emitting region of GRBs (Ackermann et al. 2014). Previous results have also pointed to there being a correlation between variability time-scales and burst duration, with the time-scales of long GRBs being different from those of short GRBs (MacLachlan et al. 2013).

The variability of GRBs in the LAT’s high-energy gamma-ray range is less well-studied. Even so, the time-scale of GRB variability at LAT energies has been used by Hascoët et al. (2012) to constrain engine factors like  $\gamma - \gamma$  opacity and the Lorentz factor of outflows. The same study also found that it is not unusual for these time-scales to be on the order of a few milliseconds. Yassine et al. (2017) also calculates the variability time-scale of a long GRB, GRB 090926A, to be about 10 ms at high energies before using this value to estimate the Lorentz factor of its beam.

A common method for estimating variability at LAT energies is to measure the widths of GRB constituent pulses (Hascoët et al. 2012). In general, GRB pulses are narrower in time at higher energies than lower energies (Nemiroff 2000), which empirically indicates that GRB variability time-scales may also appear shorter at higher gamma-ray energies. GRB time-scales on the order of 1 ms have been detected in LAT data at the GeV energy scale using an autocorrelation method in photon arrival times (Nemiroff et al. 2012).

A favoured mechanism for gamma-ray production in GRBs is synchrotron radiation created by high-energy electrons being accelerated by forward shocks with turbulent magnetic fields (Preece et al. 1998). However, at the high energies detected by the LAT, photons from inverse Compton scattering – where low energy photons are upscattered by relativistic electrons – may become important. The underlying physics of gamma-ray photon creation in GRBs remains a topic of study, and it is not clear that the LAT-detected photons are produced, in general, by the same physics that produce the lower-energy GBM-detected photons (Daigne, Bošnjak & Dubus 2011). It is therefore possible that different photon creation mechanisms, if active, create different time-scales for photon bunching in high and low energy regimes.

The combination of great distance and rapid variability makes GRBs a valuable tool for exploring the potentially temporally dispersive properties of the Universe between Earth and the GRB. Theoretically, processes that could cause temporally disperse GRB photons include Lorentz-invariance violations (Sarkar 2002), weak equivalence principle violations (Gao, Wu & Mészáros 2015; Nusser 2016; Tangmatitham & Nemiroff 2019), and potentially physical mechanisms associated with cosmologically distributed dark matter, dark energy, or vacuum fluctuations (Nemiroff et al. 2012).

Following an unexpected and informal indication of sub-pulse bunching in the arrival times of high-energy photons in GRB 080916C, a formal search was initiated to explore the reality of this bunching and search for potentially similar bunchings at high energy in other LAT-detected GRBs. The five other GRBs studied were chosen for a relatively high number of LAT-detected photons, a strong initial pulse, and recorded spectroscopic redshifts – the latter

to strengthen potential cosmological implications. This study settled on three long GRBs (GRB 080916C, GRB 090926A, and GRB 131108A) and three short GRBs (GRB 090510A, GRB 140619B, and GRB 160709A), with all except GRB 140619B and GRB 160709A having spectroscopic redshifts. Section 2 of this article provides a description of the methodology employed to explore short duration bunching, while Section 3 details the results obtained through analysis. In Section 4, the results are summarized and discussed in the context of the broader research objectives.

## 2 METHODS

What is the shortest time-scale that really exists in a GRB? For GRBs that are obviously sectioned into constituent pulses, are there inherent time-scales shorter than that of the pulses? Mathematically, the shortest time-scale measurable is the time between consecutive photon arrival times, but that is not a characteristic of the GRB because it depends on the size and sensitivity of the detector.

This work attempts to find sub-pulse time-scales inherent to GRBs by a relatively simple method – smoothing a given GRB on a series of time-scales and then looking for statistically significant bunching of photon arrival times in the original GRB as compared to its smoothed versions.

### 2.1 Data preparation

The *Fermi* LAT identifies the arrival times and directions for individual high-energy photons (Fermi-Collaboration 2021). For most GRBs, the LAT records no GRB-associated events. Conversely, in rare cases, the LAT records over 100 high-energy GRB-coincident events. This work, of course, focuses on the latter. The analysis presented here analysed *Fermi* GRB data Pass 8 (Atwood et al. 2013) downloaded from the online LAT Photon, Event, and Spacecraft Data Query (Atwood et al. 2009).

*Fermi* LAT data generally comprises two distinct relevant entry types: ‘Events’ and ‘Photons,’ with capitalization here indicating data types explicitly labelled in Pass 8 files. The arrival times of both Events and Photons are measured by the *Fermi* LAT with a temporal accuracy of approximately 10  $\mu$ s (Atwood et al. 2009). Events may include charged particles, such as electrons and protons, and photons. In contrast, entries labelled as Photons are determined from attributes and trajectories within the LAT, during the Pass 8 analysis, to be most likely photons (Atwood et al. 2013).

In the current analysis, both Event and Photon entries falling within a 3° angular error circle, and nearly time-coincident with the GRB trigger time, are considered to be genuine GRB photons. Drawing from past experience with LAT-detected GRBs, 3° was chosen to be large enough to capture most GRB LAT-detected photons, but small enough to exclude most of the irrelevant background. While a generic Event occurring at a random location and time may have an ambiguous origin, Events that are both location and time coincident with a known GRB have a much higher likelihood of being GRB-related. This principle is examined in detail in Aldrich, Mukherjee & Nemiroff (2022).

The total number of Photons and Events for the different bursts used in this analysis were as follows, GRB 080916C: 321, GRB 090926A: 404, GRB 131108A: 252, GRB 090510: 287, GRB 140619B: 31, and GRB 160709A: 76.

## 2.2 Smoothing light curves

To determine the shortest time-scale  $t_{\min}$  with statistical significance in a given GRB or a portion of a GRB in LAT data, each analysed GRB was smoothed over a range of time-scales  $t_{\text{smooth}}$ . The smoothing method implemented here involved assuming a kernel density function (KDF; Epanechnikov 1969), which assigns weights to photons arriving at various positions within a sliding time-based kernel window. This sliding window is advanced along the GRB, being centred on one photon at a time with a temporal width of  $t_{\text{smooth}}$ . Summing these KDFs up creates a kernel density estimation (KDE; Härdle et al. 2004), which is utilized to generate Monte Carlo (MC) versions of the GRB smoothed over a specific time-scale. This procedure creates an effective brightness curve of the given GRB.

The primary KDF smoothing window utilized was Gaussian in shape. Therefore, each photon's arrival time was surrounded by a Gaussian KDF with a temporal width  $t_{\text{smooth}}$ . These KDFs were then summed to create the KDE (Triveri 2023). The KDEs of the GRBs were constructed using all LAT recorded photons with an arrival time within the first 1000 s following the trigger time. An MC simulation was used to set-up the statistical tests for these GRBs, with a number of random photons thrown under the selected section of the brightness curve equivalent to the number of photons in the original burst's time range. MC simulations of 1000 realizations were performed to search for photon bunching between the actual arrival times of photons in the GRB and the arrival times under the Gaussian-smoothed GRB.

To investigate potential bunching on multiple time-scales, both  $t_{\text{smooth}}$  and a potential bunching scale  $\Delta t$  were assigned a range of values, logarithmically from  $10^{-6}$  to 50 s, increasing each time by roughly a factor of 2. Specifically, the discrete time-scales employed were, in seconds,  $10^{-6}$ ,  $2 \times 10^{-6}$ ,  $5 \times 10^{-6}$ ,  $10^{-5}$ ,  $2 \times 10^{-5}$ ,  $5 \times 10^{-5}$ ,  $10^{-4}$ ,  $2 \times 10^{-4}$ ,  $5 \times 10^{-4}$ ,  $10^{-3}$ ,  $2 \times 10^{-3}$ ,  $5 \times 10^{-3}$ , 0.01, 0.02, 0.05, 0.10, 0.20, 0.50, 1, 2, 5, 10, 20, and 50.

## 2.3 Counting photons in pairs

The first method utilized here for identifying the bunching of GRB photons involved the cumulative counting of photons that were part of a pair of photons arriving within a time gap  $\Delta t$  or less. This method, referred to as a 'pair analysis,' entailed evaluating each GRB photon sequentially. Whenever a photon arrived within a pre-determined time difference  $\Delta t$  of another photon, the tally  $R$  for photon pairs was incremented.

In total, 1000 MC simulations were created for each GRB. For each  $\Delta t$ , the fraction of the number of MC runs where the number of bunched photons in the MC smoothed GRBs was greater than or equal to that of the real GRB was computed. The lowest fraction found from all  $\Delta t$  values was noted. This proceeded for all  $t_{\text{smooth}}$  values.

A significant concentration of bunched photons was deemed present if the fraction of MC GRBs having more than or the same number of bunched pairs as the real GRB was sufficiently small – occurring in less than 1 in 370 of the MC smoothed GRBs for some  $\Delta t$ . This threshold is derived from an analogous  $3\sigma$  threshold in a normal distribution. The second smallest  $t_{\text{smooth}}$  value that shows this rare bunching for any  $\Delta t$  was declared to be  $t_{\min}$  for that GRB, the estimated time-scale of minimum detectable variability.

For clarity, an example is given here. Suppose the arrival times of 100 photons for GRB 000001A were recorded by the *Fermi* LAT. An analysis showed that  $R = 10$  photons were found to be part of a pair separated by  $\Delta t < 0.1$  s, while 50 photons by  $\Delta t < 10$  s. Now, with  $t_{\text{smooth}} = 1.0$  s, this GRB's photons are reshuffled in a

way that preserves the GRB light-curve shape smoothed over 1.0 s. It is now found for this MC GRB that 4 photons are separated by  $\Delta t < 0.1$ , and 52 by  $\Delta t < 10$  s. Then a total of 1000 MC smoothed GRBs were digitally created, also with  $t_{\text{smooth}} = 1.0$  s. Considering all 1000 MC GRBs, only 2 were found to have more bunching on the  $\Delta t < 0.1$  s time-scale than the real GRB, while 998 of them had less bunching. Additionally, on the  $\Delta t = 10$  s time-scale, 400 MC GRBs had more bunching than the real GRB, and 600 had less bunching. From this it can be seen that this GRB showed significant bunching when  $t_{\text{smooth}} = 1.0$  s and  $\Delta t = 0.1$  s, but insignificant bunching on the  $\Delta t = 10$  s time-scale. It could then be concluded that GRB 000001A has significant bunching not on the  $\Delta t$  time-scale of 0.1 s, but at the  $t_{\text{smooth}}$  time-scale of 1.0 s.

Note that the  $2\sigma$  and  $3\sigma$  thresholds do not take into account the number of  $\Delta t$  trials. Each  $\Delta t$  value analysed can be considered a new trial for each  $t_{\text{smooth}}$ . However, numerous  $t_{\text{smooth}}$  values satisfied the  $\sigma$  thresholds, and consecutive  $\Delta t$  values are not fully statistically independent. Therefore, the  $\sigma$  values considered here are more suggestive of statistical significance than actual formal delimiters. To be conservative, the *second* lowest  $t_{\text{smooth}}$  value that satisfies the  $3\sigma$  threshold was considered more indicative of  $t_{\min}$ , with an error bar spanning the duration between the first and second lowest  $t_{\text{smooth}}$  with pair fraction below  $3\sigma$ .

## 2.4 Multiplying time gaps

A second method used here to detect photon bunching in GRBs is multiplying time gaps. After choosing a GRB and determining practical start and end times for arriving events, the gaps in times between photon arrival times were calculated. Now adding all of these time gaps together will just give  $(t_{\text{end}} - t_{\text{start}})$  no matter how bunched these photons are, but multiplying the gaps together gives a result  $S$  that depends on how bunched the photons are. The largest number possible from multiplying all of the time gaps together,  $S_{\text{max}}$ , occurs when the photons are uniformly spread across the detection time interval. Any deviation from this uniformity will result in a lower  $S$  value. In general, the more bunched the photon arrival times, the smaller  $S$  becomes relative to  $S_{\text{max}}$ . The variable  $S$  has analogies to both physical and informational entropy.

The analysis procedure of time gap multiplication was as follows. First, for a given real GRB, the value of  $S$  was computed. Next, the sets of 1000 MC smoothed GRBs were recalled from the pair bunching analysis, each set smoothed over a time-scale  $t_{\text{smooth}}$ . To be clear, these recalled MC-smoothed GRBs each had an assumed KDF – assumed Gaussian – from which smoothed KDEs (light curves) were generated.

For each MC GRB smoothed by  $t_{\text{smooth}}$ , a value of  $S_{\text{smooth}}$  was computed by multiplying together the gaps in times between all arrival times. To avoid numerical overflows, the cumulative product was computed in a logarithmic space – by taking the natural logarithm of all of the time gaps and adding them together. If the value of  $S$  for the real GRB was less than 1 in 370 of the  $S_{\text{smooth}}$  values for the MC smoothed GRBs, then that GRB was deemed to have significant photon bunching over this  $t_{\text{smooth}}$ . This procedure was repeated for each  $t_{\text{smooth}}$  value. Again, the second lowest value of  $t_{\text{smooth}}$  where  $S$  occurred less frequently than 1 in 370  $S_{\text{smooth}}$  values was deemed  $t_{\min}$ . The error in  $t_{\min}$  was considered to be the difference in time between the two lowest  $t_{\text{smooth}}$  values where  $S$  occurred less frequently than 1 in 370  $S_{\text{smooth}}$  values.

### 3 RESULTS

The methods and analyses of the previous section were applied to the six GRBs selected. The *Fermi* LAT photons used in this work for the GRBs analysed are shown in Figs 1 and 2.

Before presenting the results of the main bunching analyses, two preliminary results are presented that bolster known attributes of GRBs. The first is that at high energies, the onset of the GRB was really quite sudden and not just the flux peak of a longer time-symmetric train of photons. This is apparent for all six GRBs studied by inspection of Figs 1 and 2, including both long and short GRBs. Although Fig. 1 shows that there are photons that arrive well before trigger, they are noticeably less numerous than the number of photons that arrive quite late. Although this may indicate that the very early pre-trigger photons are from an unrelated cosmic background, it more surely indicates that GRBs have high-energy photons that keep arriving many seconds after trigger, even for ‘short’ GRBs.

A second preliminary result is also visible in Figs 1 and 2. There, near the time of GRBs, the LAT pass-8 data listed as ‘Events’, shown as red dots, arrive with similar times to the LAT pass-8 data listed as ‘Photons’, shown with blue diamonds. This was described previously by Aldrich et al. (2022). To be clear, Figs 1 and 2 show that LAT Events near in time and angular location to Photons are overwhelmingly likely, per Event, to signify real GRB photons.

Additionally, inspection of the photon arrival times in Fig. 2 indicates that the initial pulse for the long GRBs, at high energies, has a duration of about 20 s, while the initial pulse for the short GRBs, over the same high energies, has a duration of about 2 s.

The main results of this analysis are shown in Figs 3 and 4, with Fig. 3 summarizing results from the cumulative pair analysis, and Fig. 4 summarizing results from the multiplying time gaps analysis. The  $x$ -axes of both plots label the smoothing time  $t_{\text{smooth}}$  used to digitally generate the smoothed MC bursts. The  $y$ -axes label the fraction of smoothed GRBs that exhibited the same or greater number of bunched photons than the real burst at any  $\Delta t$ . A very low fraction at a given  $t_{\text{smooth}}$  indicates that the bunching in the real burst is significant at that smoothing time-scale.

Several things become clear from inspection of Figs 3 and 4. First, typically, when the smoothing time-scale  $t_{\text{smooth}}$  is small, a MC smoothed burst is effectively unsmoothed and so has a similar number of photons in pairs as the real GRB. This is why the fraction is near unity on the left of the plots in Figs 3 and 4.

Conversely, when the smoothing time-scale  $t_{\text{smooth}}$  is large – say near the duration of the GRB, then MC versions of the GRB are smoothed by having their photons randomized over much of the GRB. Therefore, almost any structure in the GRB is smoothed away, and the number of close MC pairs drops to below that of the real GRB. This is why the fraction is near zero on the right of the plots in Figs 3 and 4.

The upper dashed line (pink) and lower dashed line (black) in Figs 3 and 4 indicate where the results become significant at the  $2\sigma$  and  $3\sigma$  levels, respectively. The second smallest  $t_{\text{smooth}}$  value with  $3\sigma$  significance is then referred to here as the GRB’s minimum detectable time-scale from this data analysis:  $t_{\text{min}}$ . For the long GRBs, GRB 080916C, GRB 090926A, and GRB 131108A,  $t_{\text{min}}$  was found to be 0.005, 10, and 10 s, respectively. For the short GRBs studied, GRB 090510, GRB 140619B, and GRB 160709A,  $t_{\text{min}}$  was found to be 0.05, 0.01, and 20 s, respectively. Since 20 s is on the order of this short GRB’s LAT duration (Ajello et al. 2019), this  $t_{\text{min}}$  just means that no reportable inter-GRB photon bunching was detected.

The pair analysis results were checked by utilizing a uniformly flat KDF in place of the Gaussian. Time-scales for all the GRBs were

usually slightly longer with this kernel. For the long GRBs,  $t_{\text{min}} = 0.01$  s for GRB 080916C,  $t_{\text{min}} = 20$  s for GRB 090926A, and  $t_{\text{min}} = 10$  s for GRB 131108A. For the short GRBs,  $t_{\text{min}} = 0.2$  s for GRB 090510,  $t_{\text{min}} = 0.05$  s for GRB 140619B, and  $t_{\text{min}} = 20$  s for GRB 160709A. Since each kernel has its own attributes, the differences in  $t_{\text{min}}$  values should be attributed to inherent numerical variance in the KDE methodology.

The plots in Fig. 4 show the results of the time-gap multiplication analysis. In sum, for the long GRBs, GRB 080916C, GRB 090926A, and GRB 131108A,  $t_{\text{min}}$  was found to be 2, 20, and 10 s, respectively. For the short GRBs studied, GRB 090510, GRB 140619B, and GRB 160709A,  $t_{\text{min}}$  was found to be 0.05, 0.01, and 20 s, respectively.

These time-gap multiplication analysis results were also checked by utilizing a uniformly flat KDF in place of the Gaussian. Similarly, time-scales for the long GRBs were slightly shifted with this kernel, with  $t_{\text{min}} = 0.5$  s for GRB 080916C,  $t_{\text{min}} = 20$  s for GRB 090926A, and  $t_{\text{min}} = 10$  s for GRB 131108A. The time-scales for the short GRBs studied were also shifted, with  $t_{\text{min}} = 0.2$  s for GRB 090510,  $t_{\text{min}} = 0.05$  s for GRB 140619B, and  $t_{\text{min}} = 50$  s for GRB 160709A. Again, differences with the Gaussian kernel can be attributed to inherent numerical variance.

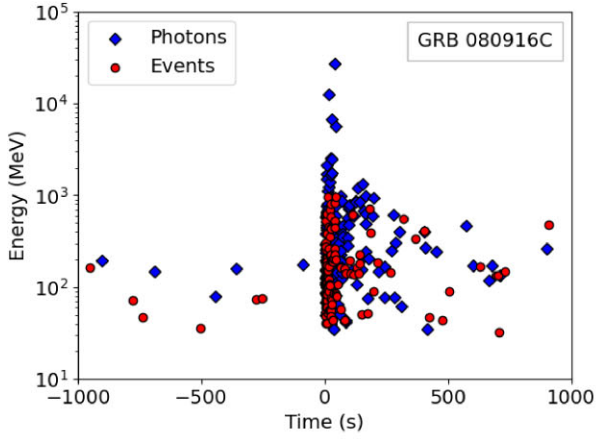
The terms  $2\sigma$  and  $3\sigma$  are used here to indicate levels of significance in familiar terms, but are not meant to indicate that the distributions of  $R$  or  $S$  are Gaussian. Classically, the numerical  $\sigma$  threshold, for example 1 in 370 for the  $3\sigma$  designation, implies significance could be obtained on either side of a two-sided Gaussian distribution curve. However in this work, significance was only searched for on one side of the distribution: the unusual bunching side and not the unusual smoothness side of photon arrival times.

### 4 DISCUSSION, SUMMARY, AND CONCLUSIONS

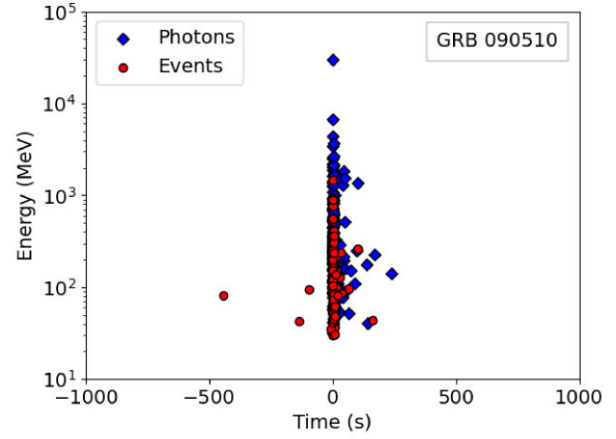
The *Fermi* LAT is particularly useful in the search for short time-scales in high-energy GRBs for at least three reasons: first because it measures so many high-energy photons from a GRB as compared to previous missions, second because the LAT records arrival times for individual photons down to the microsecond level, and third because the background at these high energies is so low that most events that occur time and space coincident with a known GRB are likely really photons associated with that GRB – and not an unrelated background. Additionally, *Fermi* is useful for detecting multiple GRBs containing over 100 LAT-detected photons, a consequence of having been active now for over 15 yr.

For short GRBs, this study found GRB high-energy variability on time-scales at or below 0.01 s for two of the short GRBs tested. This confirms the sub-0.01 s variability time-scale for GRB 090510 found exclusively at high energies by Nemiroff et al. (2012). A detailed analysis of *Fermi* data from GRB 140619B was given by Ruffini et al. (2015), but no time-scale this short was reported at high energies. GRB 160709A is less analysed (but see Augusto et al. 2018) and with no sub-0.01 s variability reported.

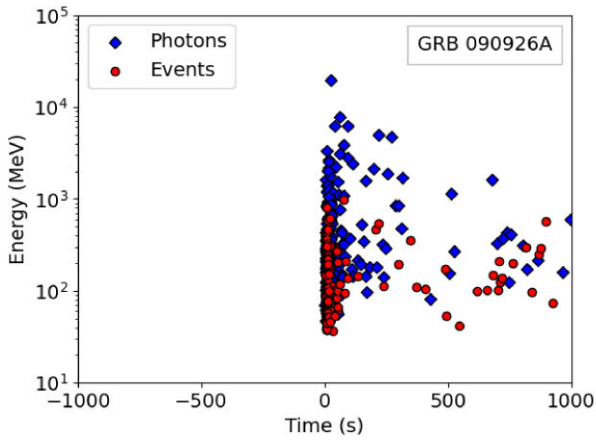
In contrast however, for long GRBs, this study found sub-0.01 s high-energy variability for only one of the three long GRBs analysed – and then only in one test: specifically the cumulative pair analysis for GRB 080916C. In contrast to Yassine et al. (2017), our analysis does not immediately confirm the 10 ms variability time-scale reported for GRB 090926A at high energies. However, Yassine et al. (2017) reported this variability time-scale for only a small portion of this GRB that was particularly fluent at high energies, so the two results could be consistent. Additionally, (Giuliani et al. 2014) reported a time-scale for GRB 131108A below 1 s for the



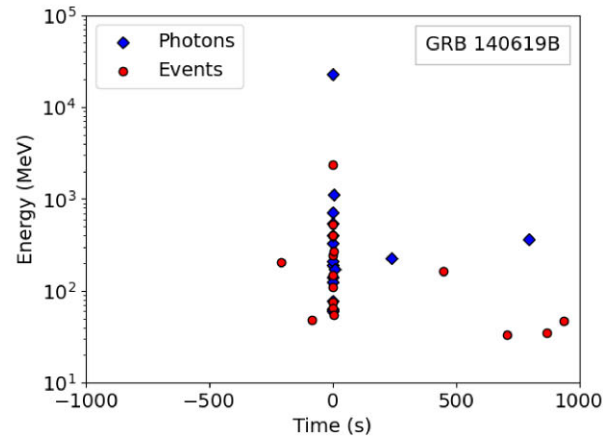
(a) GRB 080916C



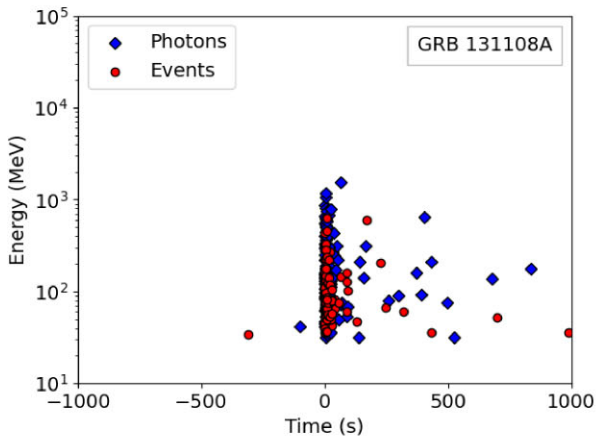
(b) GRB 090510



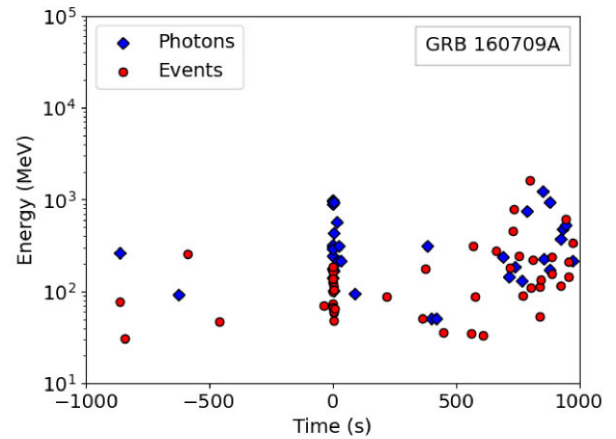
(c) GRB 090926A



(d) GRB 140619B



(e) GRB 131108A



(f) GRB 160709A

**Figure 1.** Plots of photon arrival times versus photon energy for each of the six GRBs analysed. Blue diamonds represent LAT events designated ‘Photons’, while red dots represent ‘Events’. The left three plots are for long GRBs, while the right three are for short GRBs.

initial peak. Again, our analysis for this GRB was over the entire GRB, and so may be consistent with this GRB sectional result. Stated differently, if sub-0.01 s variability existed only during a small time of the 1000 s, this variability might have been ‘averaged out’ in our analysis by the rest of the data in the complete 1000 s studied.

These results indicate that at least some short GRBs at high energies have a significantly shorter time-scale of variability than indicated by the duration of their pulses, in particular their initial pulse. More study is needed for long GRBs.

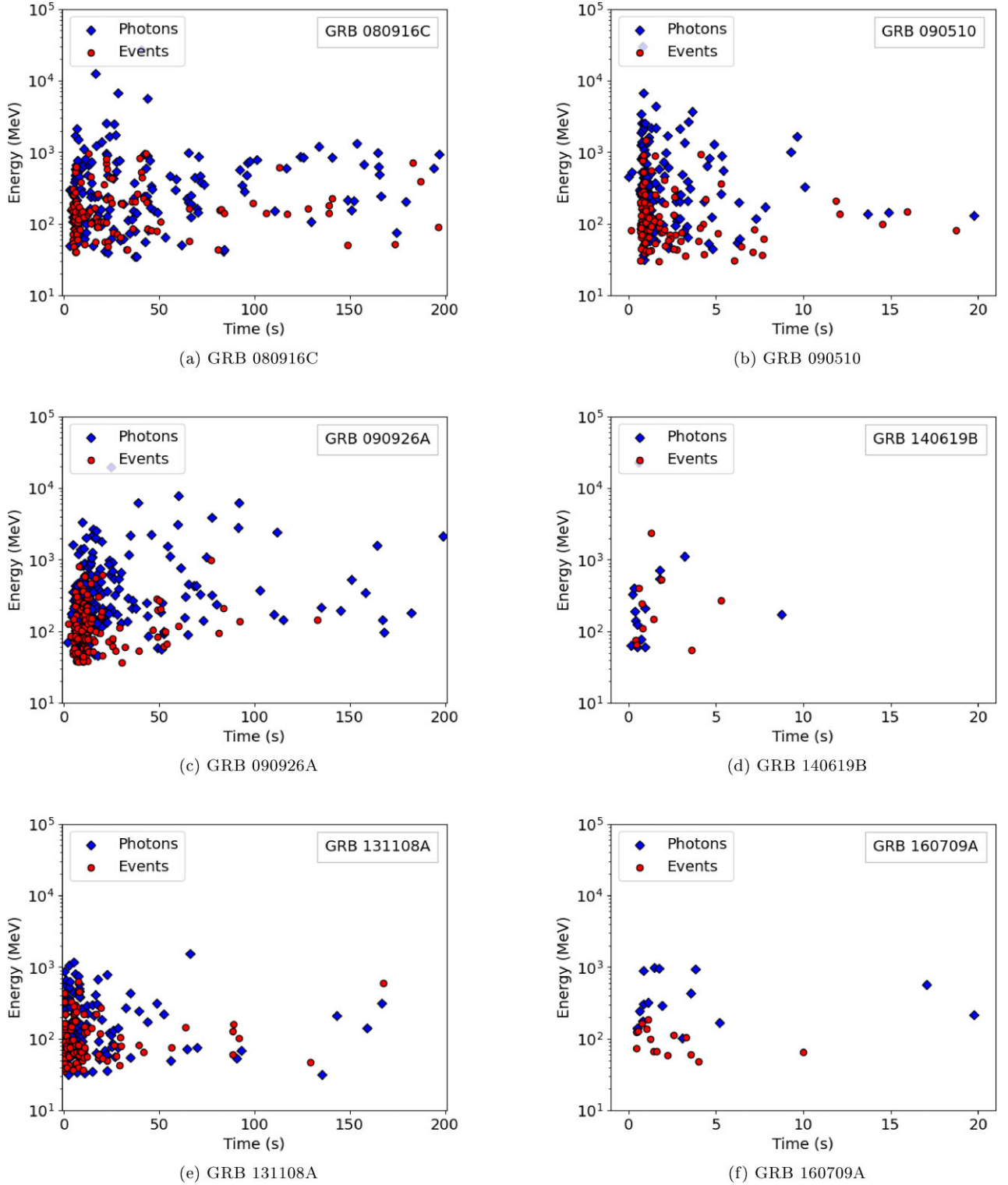
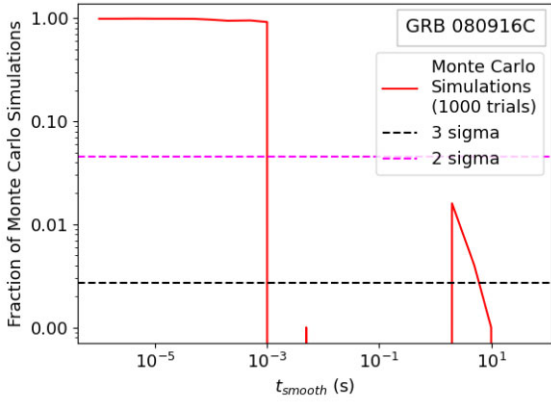


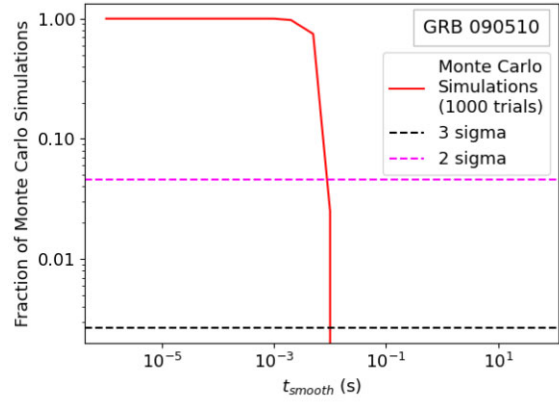
**Figure 2.** Plots of photon arrival times versus photon energy for each of the six GRBs analysed as shown in Fig. 1, but over a shorter temporal period near trigger to show earlier times more clearly.

It is interesting to note that this study was capable of detecting high-energy GRB variability down to the time-scale of microseconds – but did not. That ‘only’ a super-millisecond time-scale was found might be taken as an indication that even shorter time-scales don’t exist. However, the lack of such a short time-scale signal may also

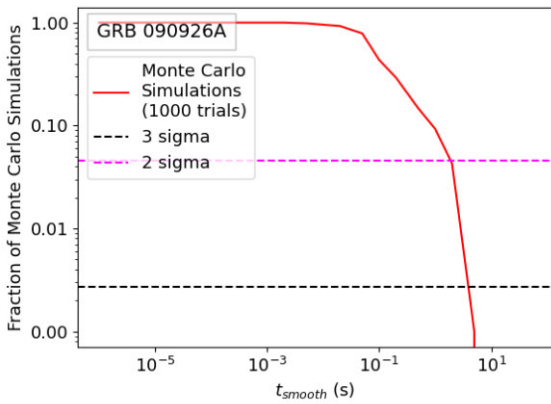
indicate that such a signal is so rare that an insufficient number of photons were processed to detect it. It also may indicate that such time-scales only existed during a small part of the GRB and was not found with the present analysis because its statistical significance was diminished over the longer parts of the GRB. Future testing may



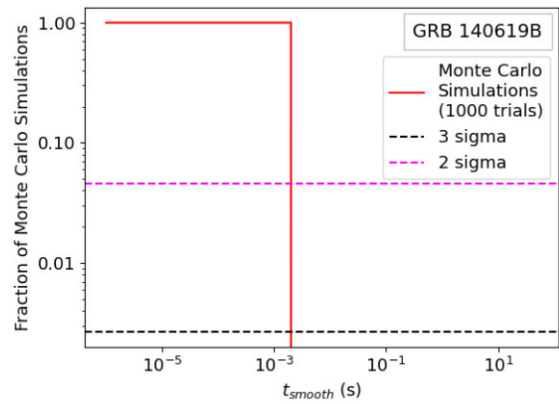
(a) GRB 080916C



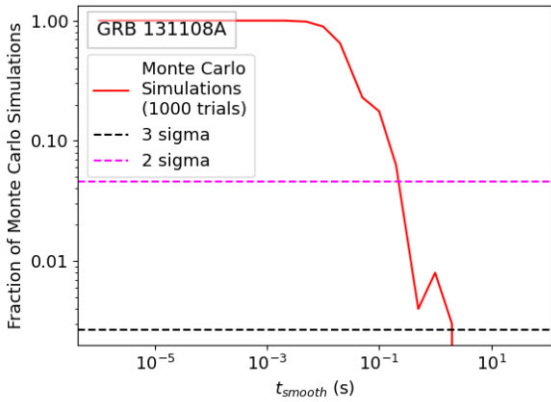
(b) GRB 090510



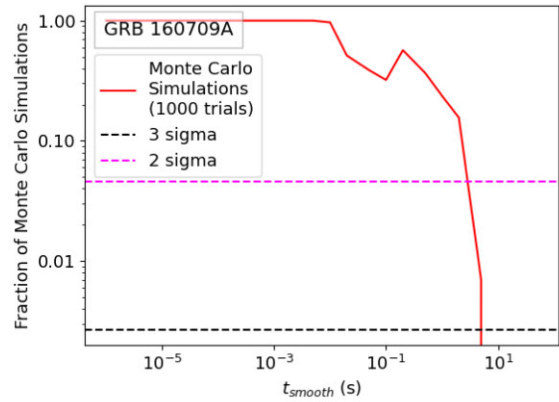
(c) GRB 090926A



(d) GRB 140619B



(e) GRB 131108A



(f) GRB 160709A

**Figure 3.** Plots showing the fraction of the 1000 MC GRBs that were bunched on a smaller time-scale than the real GRB in the photon pair test. The time-scale of smoothing  $t_{\text{smooth}}$  is shown on the x-axis. The fraction plotted is the lowest fraction at any  $\Delta t$  value compared.

probe smaller time-scales by not only analysing a greater sample of GRBs, but also by analysing GRBs with greater numbers of high-energy photons, or concentrating on smaller GRB sections in a statistically unbiased manner.

The non-detection of photon counts, particularly at the highest energies where the LAT sensitivity drops, potentially limits the possibility of finding even shorter duration variability at even higher

energies, a region of parameter space that is particularly interesting because, in general, GRBs are increasingly variable at higher energies over most of *Fermi*'s energy range (Nemiroff 2000).

The detected short-time-scale signal for short GRBs may have implications regarding the internal physics of GRB photon emission as well as temporally dispersive properties of the universe between *Fermi* and the GRB source. As with previously discovered millisecond-

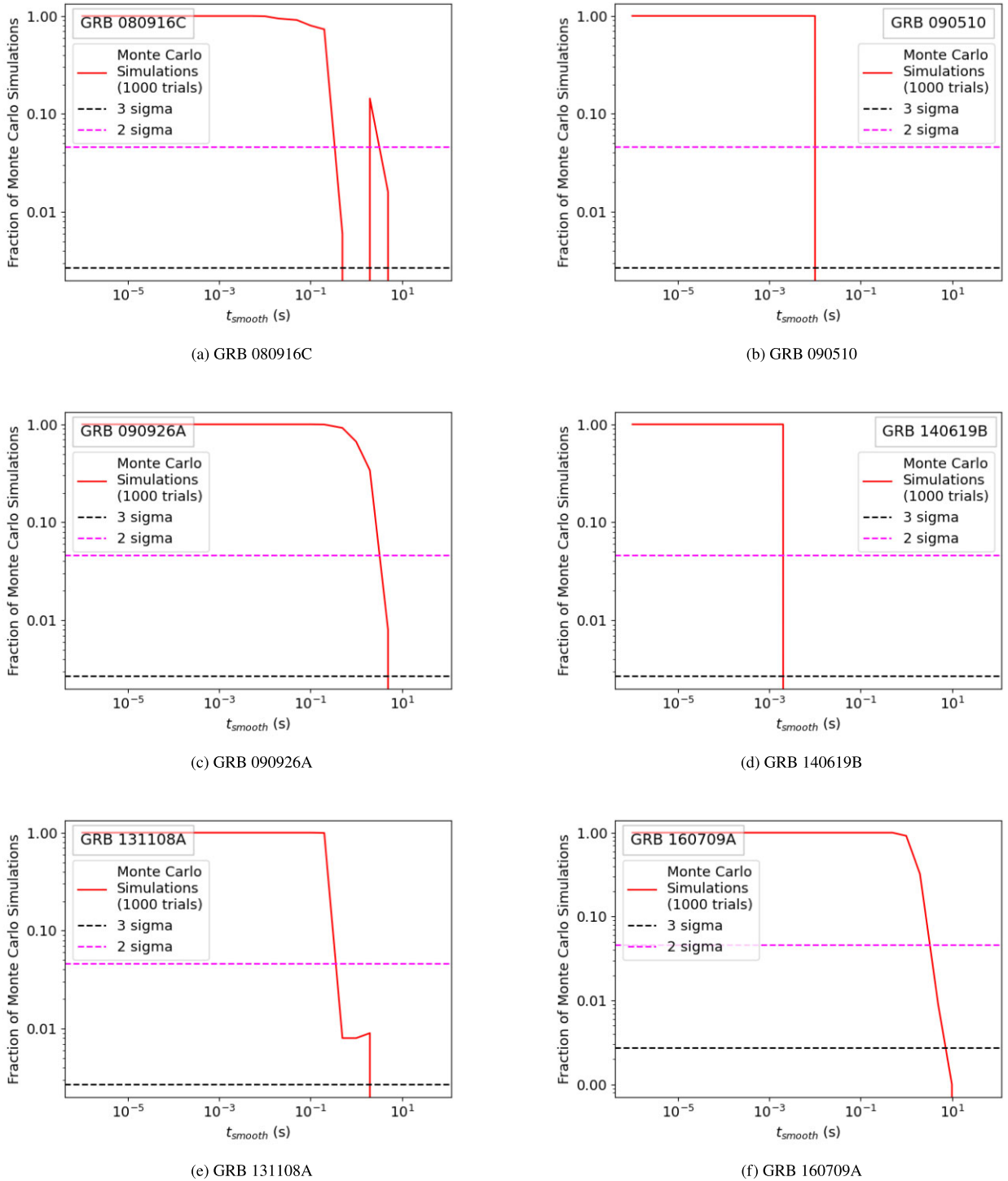


**Figure 4.** Plots showing the fraction of the 1000 MC GRBs that were bunched on a smaller time-scale than the real GRB according to the time-gap multiplication test. The time-scale of smoothing  $t_{\text{smooth}}$  is shown the  $x$ -axis.

and variability in GRBs, that photons cross the universe in such tight bunches without greater temporal dispersion can be used to probe and limit potential dispersion mechanisms in the intervening universe, including Lorentz-invariance violations, gravitational weak equivalence principle violations, and the nature of pervasive cosmological dark energy.

#### CODE AVAILABILITY

The codes underlying this article are available from GitHub at <https://github.com/ECaseyAldrich/Rapid-GRB-Variability>.

## ACKNOWLEDGEMENTS

We thank Michigan Technological University for support during this research. We thank Oindabi Mukherjee for helpful comments. We acknowledge using ChatGPT to help clarify the language in parts of the text, which was later checked for scientific accuracy by the authors. ChatGPT was also used to take existing code and optimize it for speed, which was also checked for accuracy against pre-optimized code results.

## DATA AVAILABILITY

The data underlying this article are available generally from the NASA *Fermi* website at <https://fermi.gsfc.nasa.gov/cgi-bin/ssc/LAT/LATDataQuery.cgi> and specifically formatted for the codes used in this article from GitHub at <https://github.com/ECCaseyAldrich/Rapid-GRB-Variability/tree/main/Photon%20Lists%20Used>.

## REFERENCES

- Ackermann M. et al., 2013, *ApJS*, 209, 11  
 Ackermann M. et al., 2014, *Science*, 343, 42  
 Ajello M. et al., 2019, *ApJ*, 878, 52  
 Aldrich E. C., Mukherjee O., Nemiroff R. J., 2022, *Res. Notes Am. Astron. Soc.*, 6, 237  
 Atwood W. B. et al., 2009, *ApJ*, 697, 1071  
 Atwood W. et al., 2013, 2012 Fermi Symposium proceedings - eConf C121028, preprint ([arXiv:1303.3514](https://arxiv.org/abs/1303.3514))  
 Augusto C. R. A., Navia C. E., de Oliveira M. N., Nepomuceno A., Kopenkin V., Sinzi T., 2018, *J. Phys. Commun.*, 2, 075013  
 Bhat P. N., Fishman G. J., Meegan C. A., Wilson R. B., Brock M. N., Paciasas W. S., 1992, *Nature*, 359, 217  
 Cucchiara A. et al., 2011, *ApJ*, 736, 7  
 Daigne F., Bošnjak Ž., Dubus G., 2011, *A&A*, 526, A110  
 Desai U. D., 1981, *Ap&SS*, 75, 15  
 Eichler D., Livio M., Piran T., Schramm D. N., 1989, *Nature*, 340, 126  
 Epanechnikov V. A., 1969, *Theory Probab. Appl.*, 14, 153  
 Fermi-Collaboration, 2021, in Myers J.D., Ed., NASA Goddard Space Flight Center. Overview of the LAT, [https://fermi.gsfc.nasa.gov/ssc/data/analysis/documentation/Cicerone/Cicerone\\_Introduction/LAT\\_overview.html](https://fermi.gsfc.nasa.gov/ssc/data/analysis/documentation/Cicerone/Cicerone_Introduction/LAT_overview.html) Accessed in 2021  
 Gao H., Wu X.-F., Mészáros P., 2015, *ApJ*, 810, 121  
 Giuliani A. et al., 2014, preprint ([arXiv:1407.0238](https://arxiv.org/abs/1407.0238))  
 Greiner J. C., 2024, GRBs localized, Max Plank Institute for Extraterrestrial Physics, <https://www.mpe.mpg.de/~jcg/grbgen.html> Accessed in 2021  
 Hascoët R., Daigne F., Mochkovitch R., Vennin V., 2012, *MNRAS*, 421, 525  
 Härdle W. K., Müller M., Sperlich S., Werwatz A., 2004, Nonparametric and Semiparametric Models, Springer Series in Statistics, 1. Springer Berlin, Heidelberg, Chapter 3: Nonparametric Density Estimation  
 Kouveliotou C., Meegan C. A., Fishman G. J., Bhat N. P., Briggs M. S., Koshut T. M., Paciasas W. S., Pendleton G. N., 1993, *ApJ*, 413, L101  
 Levan A., 2018, in Vishniac E., Ed., Gamma-Ray Bursts. IOP Publishing, Temple Circus, Temple Way, Bristol, BS1 6HG, UK  
 MacLachlan G. A., Shenoy A., Sonbas E., Dhuga K. S., Eskandarian A., Maximon L. C., Parke W. C., 2012, *MNRAS*, 425, L32  
 MacLachlan G. A. et al., 2013, *MNRAS*, 432, 857  
 Nemiroff R. J., 2000, *ApJ*, 544, 805  
 Nemiroff R. J., 2012, *MNRAS*, 419, 1650  
 Nemiroff R. J., Connolly R., Holmes J., Kostinski A. B., 2012, *Phys. Rev. Lett.*, 108, 231103  
 Norris J. P., Bonnell J. T., Nemiroff R. J., Scargle J. D., Kouveliotou C., Paciasas W. S., Meegan C. A., Fishman G. J., 1995, *ApJ*, 439, 542  
 Norris J. P., Nemiroff R. J., Bonnell J. T., Scargle J. D., Kouveliotou C., Paciasas W. S., Meegan C. A., Fishman G. J., 1996, *ApJ*, 459, 393  
 Nusser A., 2016, *ApJ*, 821, L2  
 Piran T., 2004, *Rev. Mod. Phys.*, 76, 1143  
 Preece R. D., Briggs M. S., Malozzi R. S., Pendleton G. N., Paciasas W. S., Band D. L., 1998, *ApJ*, 506, L23  
 Ruffini R. et al., 2015, *ApJ*, 808, 190  
 Ryde F., Svensson R., 2002, *ApJ*, 566, 210  
 Sarkar S., 2002, *Mod. Physics Letters A*, 17, 1025  
 Schaefer B. E., 1999, *Phys. Rev. Lett.*, 82, 4964  
 Shahmoradi A., Nemiroff R. J., 2015, *MNRAS*, 451, 126  
 Tangmatitham M., Nemiroff R. J., 2019, preprint ([arXiv:1903.05688](https://arxiv.org/abs/1903.05688))  
 Triveri J., 2023, Kernel Density Estimation from Scratch in Python, The Pleasure of Finding Things Out: A blog by James Triveri, <https://www.jtrive.com/kernel-density-estimation-from-scratch-in-python.html> Accessed in 2023  
 Walker K. C., Schaefer B. E., Fenimore E. E., 2000, *ApJ*, 537, 264  
 Woosley S. E., Bloom J. S., 2006, *ARA&A*, 44, 507  
 Yassine M., Piron F., Mochkovitch R., Daigne F., 2017, *A&A*, 606, A93  
 Zitouni H., Guessoum N., AlQassimi K. M., Alaryani O., 2018, *Ap&SS*, 363, 223

This paper has been typeset from a  $\text{\TeX}/\text{\LaTeX}$  file prepared by the author.